Adsorption (2013) 19:331–338
DOI 10.1007/s10450-012-9455-6

In situ SAXS investigation of dibromomethane adsorption in ordered mesoporous silica

Evangelos P. Favvas · Konstantinos L. Stefanopoulos · Achilles Vairis · John W. Nolan · Karsten D. Joensen · Athanasios C. Mitropoulos

Received: 22 October 2012 / Accepted: 7 December 2012 / Published online: 3 January 2013

Abstract A SAXS/WAXS apparatus with the aid of a specially designed sample cell capable for performing both SAXS and WAXS experiments was used for adsorption studies in nanoporous materials. The applicability of the instrument for structural investigations and its ability for adsorption experiments because of the advanced sample environment were demonstrated by carrying out *in situ* SAXS measurements during gas physisorption. SAXS profiles of ordered mesoporous silica were measured at selected equilibrium points alongside a dibromomethane (CH_2Br_2) adsorption isotherm at 293 K. SBA-15 was the adsorbent of choice because it consists of a regular 2D hexagonal array of cylindrical mesopores that gives rise to Bragg reflections in the small-angle regime. CH_2Br_2 was selected as a contrast-matching fluid because it has almost the same electron density as silica. We obtained high-quality data comparable to those resulting from experiments performed in synchrotron light sources which produce intense beams of x-rays and support advanced instrumentation for high-resolution diffraction and SAXS studies. The Bragg peaks of the pore lattice are clearly visible for the evacuated sample and at the early stages of the adsorption process. The intensity decrease and the elimination of the Bragg peaks for the saturated sample suggest that an almost perfect contrast matching was achieved. A model has been used for monitoring the fluid condensation and evaporation regime in SBA-15 by taking into account both the Bragg scattering and the diffuse scattering for spatially random pore filling. The results show the absence of spatial correlations between filled pores suggesting random pore filling.

Keywords SAXS/WAXS · Adsorption cell · In situ · SBA-15 · Hysteresis loop · Condensation/evaporation

E.P. Favvas (✉) · K.L. Stefanopoulos
Institute of Physical Chemistry, NCSR Demokritos, Ag. Paraskevi Attikis, 153 40, Athens, Greece
e-mail: favvas@chem.demokritos.gr

K.L. Stefanopoulos (✉)
e-mail: stefan@chem.demokritos.gr

A. Vairis
Department of Mechanical Engineering, Crete Institute of Technology, Estavromenos, Heraklion, 710 04, Greece

E.P. Favvas · J.W. Nolan · A.C. Mitropoulos
Department of Petroleum & Natural Gas Technology, Cavala Institute of Technology, Ag. Loukas, 654 04, Cavala, Greece

K.D. Joensen
SAXSLAB ApS., Gl. Skovlundevej 54, 2740, Skovlunde, Denmark

1 Introduction

Membranes, powders, catalysts and surfactants are some materials with various applications in the chemical and petrochemical industries. A common property of these materials is their porous structure, which is commonly produced by compaction, desiccation, aggregation, chemical decomposition, etc. Adsorption measurements (Gregg and Sing 1982), are abundantly used for the characterization of porous solids by providing information on their structural properties such as surface area, pore volume, pore size distribution, etc. Porous materials with ordered pore structure have received increasing interest because of their potential application in the fields of electronics, photonics and life sciences (Hoa et al. 2006). Further, characterization of those materials resulted in a better understanding of the adsorption mechanism because of their simple geometries and their well-defined pore sizes (Thommes et al. 2006;

Thommes 2010). This has also lead to the development of microscopic approaches such as non-local density functional theory (NLDFT) (Tarazona et al. 1987; Neimark et al. 2000) and Grand Canonical Monte Carlo (GCMC) simulation (Gelb et al. 1999). The theoretical models have been accompanied by the progress made in the development of advanced experimental techniques such as small-angle scattering of neutrons or x-rays (SANS or SAXS) (Porod 1982; Ramsay 1998; Mitropoulos et al. 1998a; Makri et al. 2000; Hoinkis et al. 2004), contrast-matching SANS (Steriotis et al. 2002a; Calo and Hall 2004; Lelong et al. 2007; Mergia et al. 2010; Stefanopoulos et al. 2011) and adsorption in conjunction with neutron (x-ray) diffraction or SANS (SAXS) (Li et al. 1994; Ramsay and Hoinkis 1998; Mitropoulos et al. 1998b; Steriotis et al. 2002b, 2004; Sel et al. 2007; Muroyama et al. 2008; Mascotto et al. 2009) which have been proved to be essential tools for elucidating the microstructure of nanoporous materials, the adsorption mechanism and the properties of confined phases within the pores. The enhanced information obtained by such combined methods has motivated the development of several adsorption *in situ* scattering set-ups and cells by controlling temperature and pressure (Mitropoulos et al. 1995; Hoinkis 1996; Katsaros et al. 2000; Kim et al. 2005; Kolhbrecher et al. 2007; Kubota et al. 2007; Zickler et al. 2007; Steriotis et al. 2008).

In this work we developed an adsorption specimen cell, appropriate for *in situ* SAXS and wide-angle x-ray scattering (WAXS) experiments. The applicability of the instrument for adsorption studies with the aid of the integrated adsorption cell was tested by carrying out *in situ* SAXS and CH_2Br_2 adsorption on ordered mesoporous silica SBA-15. The quality of the SAXS profiles is discussed and compared with those obtained from *in situ* experiments performed in synchrotron sources. Further, the results were analyzed according to a model for spatially random pore filling.

2 Experimental

2.1 Materials

SBA-15 silica was synthesized by using the technical-grade triblock copolymer Pluronic 123 as the structure-directing template in aqueous H_2SO_4 solution, and tetraethyl orthosilicate (TEOS) as the silicate source (Zhao et al. 1998). The synthesis, hydrothermal treatment and calcination of the material followed a similar protocol described in the literature (Hofmann et al. 2005).

2.2 Cell description

The developed adsorption cell, capable of operating at pressures from high vacuum up to 2 bar and at temperatures varying between $233 < T < 373$ K, allows for *in situ* gas (vapor) adsorption and WAXS/SAXS studies on powdered samples (Fig. 1b). The cell is made of stainless steel (AISI 306) and is securely locked inside a chamber under vacuum (Fig. 2); its window can be equipped by foils transparent to x-rays such as mica, quartz or kapton polyimide. The specimen cell comprises of two separate parts that are secured with M6 bolts, to ensure a tight sealing of the two parts - this enables the application of pressure to a rubber O-ring that maintains the necessary vacuum ($\sim 10^{-4}$ Torr) for adsorption.

The top part of the cell (Fig. 1a) is in the form of a two-stepped disk, it has an aperture of diameter 4.1 mm allowing for the passage of radiation. The exterior of the central aperture in the top section has a larger diameter (32 mm), tapering to a conic shape. This widespread conic modulation gives the ability for carrying out not only SAXS but also WAXS adsorption experiments without any parasitic scattering. In the case of a WAXS experiment the signal is recorded by an image plate positioned in the sample chamber (Fig. 2). Despite the small sample-plate distance, this innovative conic design of the cell allows for covering all

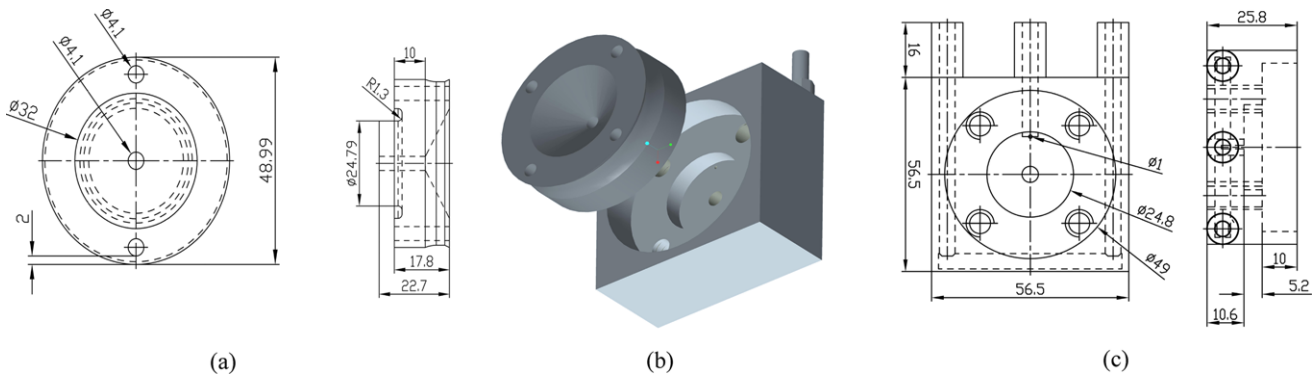

Fig. 1 (**a**) Design of the top part of the specially designed adsorption cell, (**b**) representation of the setting of the two cell parts and (**c**) design of the bottom part

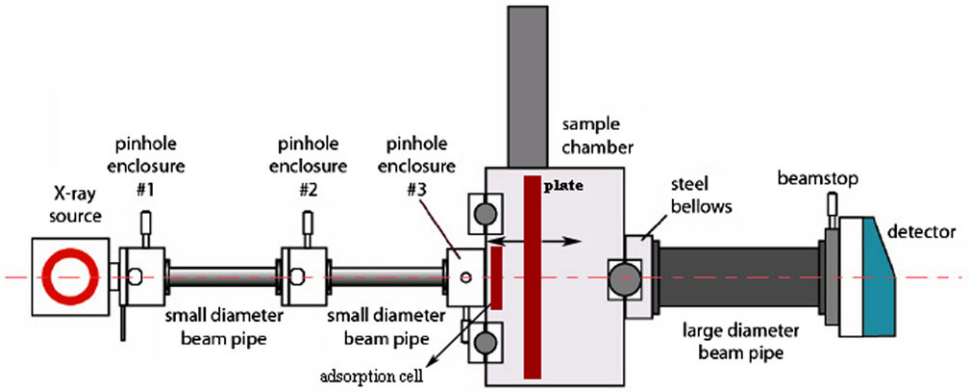

Fig. 2 SAXS/WAXS set-up apparatus. The adsorption cell is in alignment with x-rays. In the case of WAXS experiments a specific image plate is used for the recording of scattered x-rays

the available scattering angles obtained from the integration of image plate recordings.

The bottom part of the adsorption cell (Fig. 1c) houses the specimen holder area, which has an outlet for degassing the specimen and maintaining the required vacuum for the adsorption measurements. The powder specimen holder area has a useful depth of 2.5 mm and a diameter of 24.8 mm. The middle pipeline ends to an aperture (1 mm) and connects the sample cell to the adsorbate reservoir (Fig. 1c). A pressure transmitter is also joined and aligned with the central aperture. The bottom part of the specimen cell has an embedded pipe that runs around the sample holder chamber. Fluid circulation controls the temperature for the performance an isothermal adsorption experiment. Further, the internal flow system is connected to a temperature-controlled bath; when the isothermal temperature is attained, a continuous flow ensures an error of less than 0.1 K. As a further step, we are planning the integration of the SAXS/WAXS facility with our homemade gravimetric rig, as described in the following section, for obtaining adsorption isotherms simultaneously.

2.3 Experimental procedures

The N_2 adsorption isotherm has been performed volumetrically at 77 K on an Autosorb-1 gas analyzer, Micropore version (Quantachrome instruments). For adsorption measurements, the sample was initially outgassed at 300 °C for 12 h under high vacuum ($<10^{-6}$ mbar).

The CH_2Br_2 adsorption isotherm was obtained using a homemade stainless steel gravimetric rig at 293 K. The balance head (CI Microbalances), counterweight compartment, valves and tubing of the system were thermostated in an air-circulating bath (±0.1 K), whereas the sample compartment was separately thermostated in a silicon oil bath (±0.01 K).

The specimen cell was integrated into a SAXS/WAXS system (Rigaku SMAX-300) provided by JJ X-Ray Systems, connected to a sealed tube CuKα x-ray generator. The main experimental apparatus consists of the x-ray source, three pinholes collimators, the main sample chamber, the adsorption cell, the movable plate (for WAXS experiments), the beam stop and the 2D gas detector (Fig. 2). The 3-pinhole SAXS system was operated in the medium resolution mode with 850 mm to the 120 mm-diameter gas-detector, effectively yielding a Q range of 0.01–0.3 Å^{-1} (where $Q = 4\pi \sin\theta/\lambda$ is the scattering vector, λ and 2θ are the wavelength and the scattering angle respectively). As mentioned above, the adsorption cell can also be utilized for the performance of a WAXS experiment where the scattered x-rays are recorded by an image plate positioned in the sample chamber.

At the first stage, the sample was encapsulated into the space between the two parts of the cell which were bolted together. When the cell was inserted into the sample chamber box, the two terminals pipes leading to the thermostable circulator were connected. In this set-up a Julabo FP89-ME ultra-low refrigerated circulator system was used with a temperature range of $233 < T < 373$ K. The bath circulator and the vacuum pumps were started and the required experimental conditions were achieved. During the *in situ* adsorption with SAXS measurements the samples were equilibrated, at least, for 8 h for each equilibrium pressure. The exposure time of for each pressure was 1 h resulting in scattering patterns with excellent statistics. Finally, the raw data were corrected for instrumental background and scattering of the empty cell.

3 Results and discussion

3.1 *In situ* SAXS and CH_2Br_2 adsorption

The applicability of the SAXS instrument and its abilities related to the development of the adsorption cell were tested by carrying out *in situ* SAXS measurements during CH_2Br_2 adsorption in ordered mesoporous silica SBA-15. SBA-15 was the adsorbent of choice because it consists of a 2D hexagonal array of cylindrical mesopores of uniform size (*p6mm* space group). As a result, it exhibits Bragg peaks in the small-angle regime because of the regular packing of the cylindrical pores. Further, dibromomethane was chosen as a

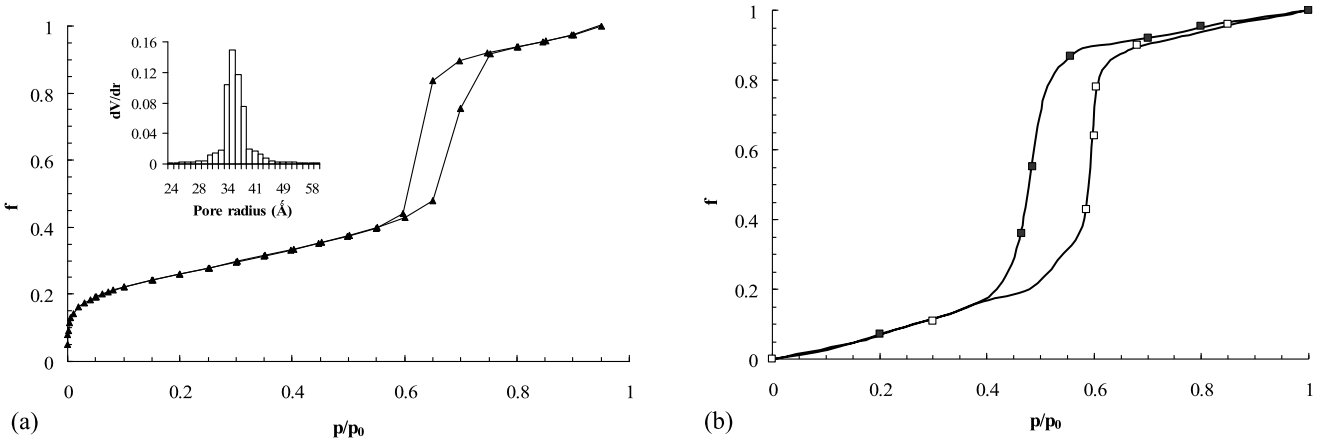

Fig. 3 Adsorption isotherms in SBA-15 silica: (**a**) nitrogen at 77 K and (*inset*) the pore size distribution calculated according to NLDFT method; (**b**) dibromomethane at 293 K (the *unfilled squares* show the isotherm adsorption points and the *filled squares* the isotherm desorption points where the SAXS measurements have been performed). f is the filling fraction, and p/p_0 is the relative vapor pressure

Table 1 Structural parameters of SBA-15 obtained by N_2 adsorption at 77 K and SAXS

Sample	S_{BET} (m^2/g)	V_p (cm^3/g)	a_0 (Å)	D_{BJH} (Å)	D_{NLDFT} (Å)	D_{FMS} (Å)
SBA-15	593	0.736	107.2	56.2	70.4	69.8

Abbreviations: S_{BET}, BET specific surface area, V_p: primary mesopore volume calculated using the α_s plot, a_0: lattice parameter estimated from the interplanar d_{100} spacing of the SAXS pattern, D_{BJH}: pore size evaluated by the BJH method, D_{NLDFT}: pore size obtained by the NLDFT method, D_{FMS}: pore size evaluated according to a recently proposed equation for accurate mesopore size calculations without the addition of the film thickness (Favvas et al. 2011)

contrast-matching fluid because it has almost the same electron density as silica.

The nitrogen (77 K) and dibromomethane (293 K) adsorption isotherms in silica SBA-15 are presented in Fig. 3. Both isotherms are of type IV, according to the IUPAC classification (Sing et al. 1985). At low relative pressures, a steep increase is observed due to the formation of a film of adsorbed molecules at the inner pore walls. At higher pressures an extended multilayer region and a sharp pore condensation step can be observed. In addition, they exhibit a hysteresis loop (type H1 by IUPAC classification) corresponding to capillary condensation and evaporation on open cylindrical pores at both ends. The different relative pressures associated with capillary condensation/evaporation regimes for the two fluids are justified by the differences in surface tension and molar volume according to the Kelvin equation (Thomson 1871). Furthermore, the amount adsorbed practically levels off at filling fraction above 0.9 as the mesopores are completely filled. The structural parameters of SBA-15 obtained by both nitrogen adsorption and SAXS measurements are presented in Table 1.

The SAXS profiles of SBA-15 measured at selected equilibrium points alongside the CH_2Br_2 adsorption/desorption cycle at 293 K are presented in Fig. 4. Up to seven Bragg diffraction peaks (10), (11), (20), (21), (30), (22) and (31) of the two-dimensional hexagonal lattice of cylindrical pores surrounding the silica matrix of SBA-15 are clearly visible for the evacuated sample and at the early stages of the adsorption process. It is worth mentioning that the quality of our results is comparable to that resulting from *in situ* experiments performed in synchrotron light sources which produce intense beams of x-rays and support advanced instrumentation for high-resolution diffraction and SAXS studies. In specific, Findenegg and co-workers obtained up to seven Bragg peaks for the SBA-15/C_5F_{12} system (Zickler et al. 2006) and up to 10 Bragg peaks for the SBA-15/CH_2Br_2 system (Jähnert et al. 2009).

The scattering signal of the main peak decreases monotonically with increasing relative pressure. When capillary condensation takes place a strong decrease of peak intensities is observed. The opposite is true during desorption where, at the onset of pore evaporation, the peak intensities are increased and the initial state is reached again suggesting the reversibility of these processes. Another interesting point is that the (21) reflection at 0.184 $Å^{-1}$ is hardly seen for the empty sample but it is clearly visible at higher relative pressures for both the adsorption and desorption process (Fig. 4). This can be attributed to the filling of the additional disorderd pores; since these pores are filled the long-range order of the pore lattice is resolved. Finally, in the case of the fully saturated sample the intensity decreases and the Bragg peaks vanish indicating that an almost perfect contrast matching was achieved.

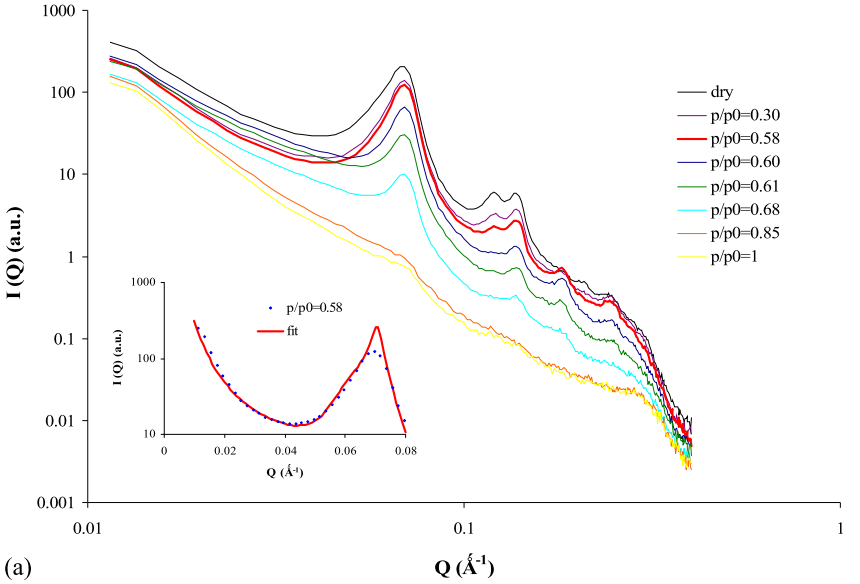

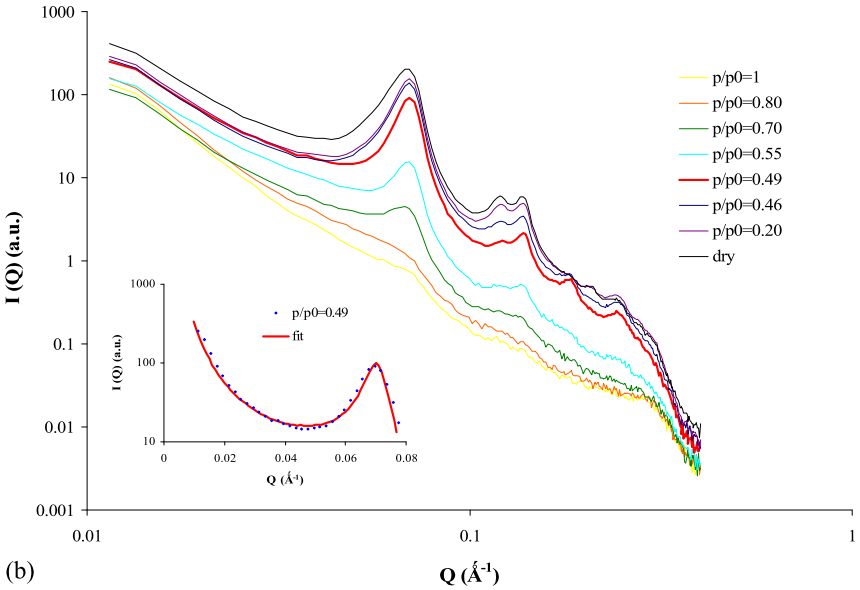

Fig. 4 (**a**) *In situ* SAXS profiles from SBA-15 during CH_2Br_2 adsorption. *Inset*: fitted SAXS curve for $p/p_0 = 0.58$. (**b**) *In situ* SAXS profiles from SBA-15 during CH_2Br_2 desorption. *Inset* fitted SAXS curve for $p/p_0 = 0.49$

3.2 Data analysis

The *in situ* SAXS data from SBA-15 have been treated according to an analytical model which considers both the contribution of the Bragg scattering and the diffuse scattering for spatially random pore filling (Erko et al. 2010). In brief, the diffuse scattering intensity, I_{Diffuse}, is given by the so called Laue scattering:

$$I_{\text{Diffuse}}(Q,\gamma) = K\frac{|F(Q)|^2}{Q}\gamma(1-\gamma) \tag{1}$$

where K is a constant, $|F(Q)|^2/Q$ is the spherically averaged form factor of a single cylindrical pore, Q is the scattering vector and γ is the fraction of completely filled pores given by:

$$\gamma = (f - f_0)/(1 - f_0) \tag{2}$$

where f is the absolute pore-filling fraction describing the adsorption isotherm and f_0 is the amount of fluid in the adsorbed film in the not yet condensed pores. One may then assume that the thickness of the adsorbed film remains unchanged during condensation and evaporation. This means

that during the capillary condensation and evaporation processes the system is assumed to consist of filled (fraction γ) and multilayer-covered empty pores (fraction f_0). Further, the Bragg scattering intensity, I_{Bragg}, is the product of the single form factor and the structure factor of the scattering objects, also multiplied by the factor $(1-\gamma)^2$ that denotes the intensity decrease upon random filling of the pores:

$$I_{\mathrm{Bragg}}(Q,\gamma) = K\left|F(Q)\right|^2 \frac{S(Q)}{Q^2}(1-\gamma)^2 \tag{3}$$

where $S(Q)/Q^2$ is the spherically averaged structure factor of the pore lattice.

The contribution of grain scattering which is dominant at low Q has been taken into account by considering the scattering profile from the sample entirely filled with dibromomethane. The model has been applied for SAXS profiles measured along the hysteresis loop of the isotherm, i.e. within the capillary condensation/evaporation regime. As a result, micropore filling is not expected to influence the results, since micropores are almost completely filled before mesopore capillary condensation commences (Jähnert et al. 2009; Müter et al. 2009). The scattering curves were fitted according to the summation of Eq. (1) and Eq. (3) respectively where γ was the only free parameter. For the evaluation of the form factor the expression of a circular pore cross section was used while the structure factor was approximated by a pseudo-Voigt function (Erko et al. 2010).

The experimental data can be perfectly described by the model suggesting a random pore filling and pore emptying according to Kelvin equation (Fig. 4; insets). Figure 5 shows the linear relationship over the whole condensation and evaporation range between the filling fraction f determined by the adsorption isotherm and the fraction γ of filled pores as obtained from the model fits. The result confirms the assumption of a constant film thickness during capillary condensation and evaporation ($f_0 = 0.27$). Application of the model to SANS results of water and perfluoropentane (C_5F_{12}) adsorption in SBA-15 also suggested a non-correlated pore-filling process in SBA-15 (Erko et al. 2010). Further, except for the water desorption, f_0 differed only slightly for the two fluids for both desorption and adsorption branches ($f_0 \sim 0.33$) in fully line with our results. For the water desorption, however, the small value of f_0 ($f_0 = 0.06$) was attributed to different fluid-fluid versus fluid-wall interactions. Conclusively, our results confirm the random pore filling in ordered mesoporous silica by using another adsorbate (CH_2Br_2) and a sample (SBA-15) with smaller values of surface area, pore volume and pore size compared to that used in the previous study (Erko et al. 2010).

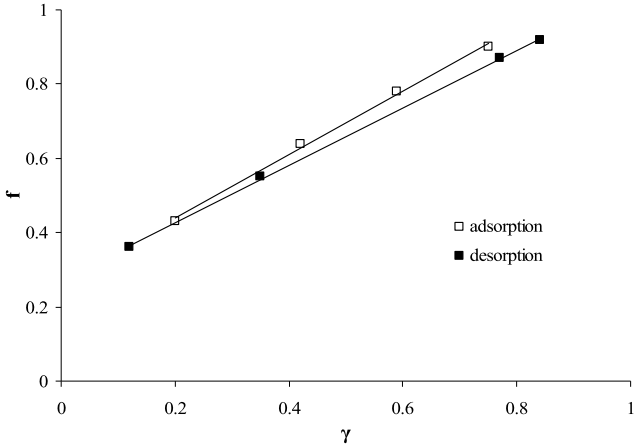

Fig. 5 Pore-filling fraction f (determined from the adsorption isotherm) versus the fraction of completely liquid filled pores γ (determined from the SAXS fits). *Straight lines* are fits to the data. See text for details

4 Conclusions

The applicability of our SAXS/WAXS apparatus for adsorption studies is demonstrated by carrying out *in situ* SAXS experiments and CH_2Br_2 adsorption in ordered mesoporous silica alongside an isothermal adsorption/desorption cycle at 293 K. For this purpose, a specially designed sample cell was constructed appropriate for the performance of both SAXS and WAXS experiments. We obtained high-quality data comparable to those resulting from synchrotron x-ray diffraction and SAXS experiments. The *in situ* SAXS profiles within the fluid condensation and evaporation regime (hysteresis loop) in SBA-15 are satisfactorily described by a model which takes into account both the contributions of Bragg and diffuse scattering. The results show that there are no spatial correlations between filled pores during capillary condensation and evaporation.

Acknowledgements The authors would like to acknowledge Thalis "NANOCAPILLARY MIS 375233" research project of the Greek Ministry of National Education and Religious Affairs for the funding of the present study.

References

Calo, J.M., Hall, P.J.: The application of small angle scattering techniques to porosity characterization in carbons. Carbon **42**, 1299–1304 (2004)

Erko, M., Wallacher, D., Brandt, A., Paris, O.: In-situ small-angle neutron scattering study of pore filling and pore emptying in ordered mesoporous silica. J. Appl. Crystallogr. **43**, 1–7 (2010)

Favvas, E.P., Stefanopoulos, K.L., Mitropoulos, A.C.: A simple equation for accurate mesopore size calculations. Microporous Mesoporous Mater. **145**, 9–13 (2011)

Gelb, L.D., Gubbins, K.E., Radhakrishnan, R., Sliwinska-Bartkowiak, M.: Phase separation in confined systems. Rep. Prog. Phys. **62**, 1573–1659 (1999)

Gregg, S.J., Sing, K.S.W.: Adsorption, Surface Area and Porosity. Academic Press, London (1982)

Hoa, M.L.K., Lu, M., Zhang, Y.: Preparation of porous materials with ordered hole structure. Adv. Colloid Interface Sci. **121**, 9–23 (2006)

Hofmann, T., Wallacher, D., Huber, P., Birringer, R., Knorr, K., Schreiber, A., Findenegg, G.H.: Small-angle x-ray diffraction of Kr in mesoporous silica: effects of microporosity and surface roughness. Phys. Rev. B **72**, 064122 (2005)

Hoinkis, E.: Small angle neutron scattering study of C_6D_6 condensation in a mesoporous glass. Langmuir **12**, 4299–4302 (1996)

Hoinkis, E., Lima, E.B.F., Schubert-Bischoff, P.: A study of carbon black corax N330 with small-angle scattering of neutrons and x-rays. Langmuir **20**, 8823–8830 (2004)

Jähnert, S., Müter, D., Prass, J., Zickler, G.A., Paris, O., Findenegg, G.H.: Pore structure and fluid sorption in ordered mesoporous silica. I. Experimental study by in situ small-angle x-ray scattering. J. Phys. Chem. C **113**, 15201–15210 (2009)

Katsaros, F.K., Steriotis, T.A., Stefanopoulos, K.L., Kanellopoulos, N.K., Mitropoulos, A.C., Meissner, M., Hoser, A.: Neutron diffraction study of adsorbed CO_2 on a carbon membrane. Physica B **276–278**, 901–902 (2000)

Kim, M.-H., Glinka, C.J., Carter, R.N.: In situ vapor sorption apparatus for small-angle neutron scattering and its application. Rev. Sci. Instrum. **76**, 113904 (2005)

Kolhbrecher, J., Bollhalder, A., Vavrin, R., Meier, G.: A high pressure cell for small angle neutron scattering up to 500 MPa in combination with light scattering to investigate liquid samples. Rev. Sci. Instrum. **78**, 125101 (2007)

Kubota, Y., Takata, M., Kobayashi, T.C., Kitagawa, S.: Observation of gas molecules adsorbed in the nanochannels of porous coordination polymers by the in situ synchrotron powder diffraction experiment and the MEM/Rietveld charge density analysis. Coord. Chem. Rev. **251**, 2510–2521 (2007)

Lelong, G., Price, D.L., Brady, J.W., Saboungi, M.-L.: Dynamics of trehalose molecules in confined solutions. J. Chem. Phys. **127**, 065102 (2007)

Li, J.-C., Ross, D.K., Howe, L.D., Stefanopoulos, K.L., Fairclough, J.P.A., Heenan, R., Ibel, K.: Small angle neutron scattering studies of the fractal-like network formed during desorption and adsorption of water in porous materials. Phys. Rev. B **49**, 5911–5917 (1994)

Makri, P.K., Stefanopoulos, K.L., Mitropoulos, A.C., Kanellopoulos, N.K., Treimer, W.: Study on the entrapment of mercury in porous glasses by neutron scattering in conjunction with mercury porosimetry. Physica B **276–278**, 479–480 (2000)

Mascotto, S., Wallacher, D., Brandt, A., Hauss, T., Thommes, M., Zickler, G.A., Funari, S.S., Timmann, A., Smarsly, B.M.: Analysis of microporosity in ordered mesoporous hierarchically structured silica by combining physisorption with in situ small-angle scattering (SAXS and SANS). Langmuir **25**, 12670–12681 (2009)

Mergia, K., Stefanopoulos, K.L., Ordás, N., García-Rosales, C.: A comparative study of the porosity of doped graphites by small angle neutron scattering, nitrogen adsorption and helium pycnometry. Microporous Mesoporous Mater. **134**, 141–149 (2010)

Mitropoulos, A.C., Haynes, J.M., Richardson, R.M., Kanellopoulos, N.K.: Characterization of porous glass by adsorption of dibromethane in conjunction with small-angle x-ray scattering. Phys. Rev. B **52**, 10035 (1995)

Mitropoulos, A.C., Kanellopoulos, N.K., Stefanopoulos, K.L., Heenan, R.K.: Scattering by curved and fractal surfaces. J. Colloid Interface Sci. **203**, 229–230 (1998a)

Mitropoulos, A.C., Stefanopoulos, K.L., Kanellopoulos, N.K.: Coal studies by small angle X-ray scattering. Microporous Mesoporous Mater. **24**, 29–39 (1998b)

Muroyama, N., Yoshimura, A., Kubota, Y., Miyasaka, K., Ohsuna, T., Ryoo, R., Ravikovitch, P.I., Neimark, A.V., Takata, M., Terasaki, O.: Argon adsorption on MCM-41 mesoporous crystal studied by in situ synchrotron powder X-ray diffraction. J. Phys. Chem. C **112**, 10803–10813 (2008)

Müter, D., Jähnert, S., Dunlop, J.W.C., Findenegg, G.H., Paris, O.: Pore structure and fluid sorption in ordered mesoporous silica. II. Modeling. J. Phys. Chem. C **113**, 15211–15217 (2009)

Neimark, A.V., Ravikovitch, P.I., Vishnyakov, A.: Adsorption hysteresis in nanopores. Phys. Rev. E **62**, R1493 (2000)

Porod, G.: General theory. In: Glatter, O., Kratky, O. (eds.) Small Angle X-Ray Scattering, pp. 17–51. Academic Press, London (1982)

Ramsay, J.D.F.: Surface and pore structure characterisation by neutron scattering techniques. Adv. Colloid Interface Sci. **76–77**, 13–37 (1998)

Ramsay, J.D.F., Hoinkis, E.: SANS investigations of benzene adsorption on porous silica gel. Physica B **248**, 322–326 (1998)

Sel, O., Brandt, A., Wallacher, D., Thommes, M., Smarsly, B.: Pore hierarchy in mesoporous silicas evidenced by in-situ SANS during nitrogen physisorption. Langmuir **23**, 4724–4727 (2007)

Sing, K.S.W., Everett, D.H., Haul, R.A.W., Moscou, L., Pierotti, R.A., Rouquérol, J., Siemieniewska, T.: Reporting physisorption data for gas/solid systems with special reference to the determination of surface area and porosity. Pure Appl. Chem. **57**, 603–619 (1985)

Stefanopoulos, K.L., Romanos, G.E., Vangeli, O.C., Mergia, K., Kanellopoulos, N.K., Koutsioubas, A., Lairez, D.: Investigation of confined ionic liquid in nanostructured materials by a combination of SANS, contrast-matching SANS, and nitrogen adsorption. Langmuir **27**, 7980–7985 (2011)

Steriotis, Th.A., Stefanopoulos, K.L., Keiderling, U., De Stefanis, A., Tomlinson, A.A.G.: Characterisation of pillared clays by contrast-matching small-angle neutron scattering. Chem. Commun. **20**, 2396–2397 (2002a)

Steriotis, T.A., Stefanopoulos, K.L., Mitropoulos, A.C., Kanellopoulos, N.K., Hoser, A., Hofmann, M.: Structural studies of supercritical carbon dioxide in confined space. Appl. Phys. A, Mater. Sci. Process. **74**, S1333–S1335 (2002b)

Steriotis, Th.A., Stefanopoulos, K.L., Kanellopoulos, N.K., Mitropoulos, A.C., Hoser, A.: The structure of adsorbed CO_2 in carbon nanopores: a neutron diffraction study. Colloids Surf. A, Physicochem. Eng. Asp. **241**, 239–244 (2004)

Steriotis, Th.A., Stefanopoulos, K.L., Katsaros, F.K., Gläser, R., Hannon, A.C., Ramsay, J.D.F.: In situ neutron diffraction study of adsorbed carbon dioxide in a nanoporous material: monitoring the adsorption mechanism and the structural characteristics of the confined phase. Phys. Rev. B **78**, 115424 (2008)

Tarazona, P., Marconi, U.M.B., Evans, R.: Phase equilibria of fluid interfaces and confined fluids-non-local versus local density functionals. Mol. Phys. **60**, 573–595 (1987)

Thommes, M., Smarsly, B., Groenewolt, M., Ravikovitch, P.I., Neimark, A.V.: Adsorption hysteresis of nitrogen and argon in pore networks and characterization of novel micro- and mesoporous silicas. Langmuir **22**, 756–764 (2006)

Thommes, M.: Physical adsorption characterization of nanoporous materials. Chem. Ing. Tech. **82**, 1059–1073 (2010)

Thomson, W.: On the equilibrium of vapor at a curved surface of liquid. Philos. Mag. **42**, 448–452 (1871)

Zhao, D., Feng, J., Huo, Q., Melosh, N., Fredrickson, G.H., Chmelka, B.F., Stucky, G.D.: Triblock copolymer syntheses of mesoporous silica with periodic 50 to 300 ångstrom pores. Science **279**, 548–552 (1998)

Zickler, G.A., Jähnert, S., Wagermaier, W., Funari, S.S., Findenegg, G.H., Paris, O.: Physisorbed films in periodic mesoporous silica studied by in situ synchrotron small-angle diffraction. Phys. Rev. B **73**, 184109 (2006)

Zickler, G.A., Jähnert, S., Funari, S.S., Findenegg, G.H., Paris, O.: Pore lattice deformation in ordered mesoporous silica studied by in situ small-angle X-ray diffraction. J. Appl. Crystallogr. **40**, s522–s526 (2007)